Author Manuscript

Author Manuscript

Author Manuscript

Author Manuscript

HHS Public Access

Author manuscript

Clin Genet. Author manuscript; available in PMC 2017 March 01.

Published in final edited form as:

Clin Genet. 2016 March ; 89(3): 359–366. doi:10.1111/cge.12608.

Mutations in *RIT1* cause Noonan syndrome – additional functional evidence and expanding the clinical phenotype

Martin Koenighofer[1,*], **Christina Y. Hung**[2,*], **Jacob L. McCauley**[3], **Julia Dallman**[4], **Emma J. Back**[4], **Ivana Mihalek**[5], **Karen W. Gripp**[6], **Katia Sol-Church**[6], **Paolo Rusconi**[7], **Zhaiyi Zhang**[8], **Geng-Xian Shi**[8], **Douglas A. Andres**[8], and **Olaf A. Bodamer**[2,9]

[1]Department of Otorhinolaryngology, Medical University of Vienna, Austria

[2]Division of Genetics and Genomics, Boston Children's Hospital, Boston, MA, USA

[3]Dr. John T. Macdonald Foundation Department of Human Genetics and John P. Hussman Institute for Human Genomics, University of Miami, Miller School of Medicine, FL, USA

[4]Department of Biology, University of Miami, FL, USA

[5]Bioinformatics Institute A*STAR Singapore, Singapore

[6]Division of Medical Genetics, Alfred I. duPont Hospital for Children, Wilmington, DE, USA

[7]Division of Pediatric Cardiology, Department of Pediatrics, University of Miami, Miller School of Medicine, FL, USA

[8]Department of Molecular and Cellular Biochemistry, University of Kentucky, College of Medicine, Lexington, KY, USA

[9]Harvard Medical School, Boston, MA, USA

Abstract

RASopathies are a clinically heterogeneous group of conditions caused by mutations in one of sixteen proteins in the RAS-MAPK pathway. Recently, mutations in *RIT1* were identified as a novel cause for Noonan syndrome. Here we provide additional functional evidence for a causal role of *RIT1* mutations and expand the associated phenotypic spectrum.

We identified two *de novo* missense variants p.Met90Ile and, p.Ala57Gly. Both variants resulted in increased MEK-ERK signaling compared to wild-type, underscoring gain-of-function as the primary functional mechanism. Introduction of p.Met90Ile and p.Ala57Gly into zebrafish embryos reproduced not only aspects of the human phenotype but also revealed abnormalities of eye development, emphasizing the importance of *RIT1* for spatial and temporal organization of the

Correspondence to: Olaf A. Bodamer, MD, PhD, FACMG, FAAP; Division of Genetics and Genomics, Department of Medicine, Boston Children's Hospital, 300 Longwood Avenue, Boston MA 02115. Tel: 8572185544 Fax: 6177300466; olaf.bodamer@childrens.harvard.edu.

*these authors contributed equally

Conflict of interest: None noted for any of the authors

Ethics approval: The project was approved by the institutional review board (IRB) of the University of Miami, Miller School of Medicine (IRB #20081166).

Author Manuscript Author Manuscript Author Manuscript Author Manuscript

growing organism. In addition, we observed severe lymphedema of the lower extremity and genitalia in one patient.

We provide additional evidence for a causal relationship between pathogenic mutations in *RIT1*, increased RAS-MAPK/MEK-ERK signaling and the clinical phenotype. The mutant RIT1 protein may possess reduced GTPase activity or a diminished ability to interact with cellular GTPase activating proteins, however the precise mechanism remains unknown. The phenotypic spectrum is likely to expand and includes lymphedema of the lower extremities in addition to nuchal hygroma.

Keywords

Costello syndrome; Noonan syndrome; RASopathy; RIT1

INTRODUCTION

Germline mutations in 16 genes of the RAS-mitogen activated protein kinase (RAS-MAPK) pathway cause a clinically heterogeneous group of conditions called RASopathies. Examples of the clinical and molecular diversity include Cardio-Facio-Cutaneous syndrome (CFC, OMIM #115150) due to mutations in *BRAF*, *MAP2K1*, *MAP2K2* and *KRAS*, Costello syndrome (OMIM #218040) due to mutations in *HRAS*, and Noonan syndrome (OMIM #163950) due to mutations in *BRAF*, *CBL*, *KRAS*, *MAP2K1*, *NRAS*, *PTPN11*, *RAF1*, *SHOC2*, *SOS1*, *SOS2 and LZTR1* (1, 2). Approximately 20% of patients with a RASopathy phenotype do not have an identifiable mutation in the known, associated genes. Recently, Aoki et al. showed that gain-of-function mutations in *RIT1* cause Noonan syndrome, expanding the molecular spectrum of RASopathies (3). Additional Noonan patients with pathogenic *RIT1* mutations were reported (4–6).

The 25 kDa protein RIT1 is a small RAS-like GTPase that transitions between GTP-bound active and GDP-bound inactive states. *RIT1* is expressed ubiquitously in embryonic and adult tissues (7). It is a member of a subfamily of RAS-related small GTPases, sharing more than 50% sequence identity with other RAS-family members. The gene product interacts with common signaling cascades including the RAS-MAPK-pathway and its final effectors extracellular signal-regulated kinases 1 and 2 (ERK1/2), which play an important role in cell proliferation, differentiation and senescence (8). Like other RAS GTPases, biochemical studies revealed that RIT1 possesses selective and high affinity guanine nucleotide binding and canonical GTPase activity (7).

When expressed in developing eye and wing discs, activated forms of *Drosophila* Ric, an orthologue of the vertebrate RIT1 and RIN GTPases, promote ectopic production of wing veins and aberrant photoreceptor differentiation, which is suppressed by genetic reduction within the MAPK-ERK cascade (9). However, D-Ric null flies display no apparent defects in patterning or apoptosis in developing embryonic or larval tissues and recently generated RIT1 knockout mice do not display gross morphological or anatomical abnormalities either (9). Instead, studies in these knockout models demonstrate that RIT1 promotes survival in response to oxidative stress through activation of an evolutionarily conserved p38-AKT-

Author Manuscript Author Manuscript Author Manuscript Author Manuscript

BAD signaling cascade. The contribution of RIT1 to embryonic development remains poorly understood.

RIT1 mutants expressed in NIH3T3 cells may activate ELK1, a transcription factor activated by ERK2. Compared to wild-type transactivation of ELK1, RIT1 variants display an activity gradient most prominent with expression of p.Gln79Leu, followed by p.Gly95Ala, p.Ala57Gly, p.Pro82Leu and p.Glu81Gly. Furthermore, Aoki et al. showed that the RIT1 variant p.Ser35Thr identified in one patient increased ELK1 signaling compared to the known dominant negative mutant p.Ser35Ala, thus supporting the gain-of-function character of *RIT1* mutations in Noonan syndrome (3).

We identified 2 patients with a clinical RASopathy phenotype due to *de novo*, gain-of-function mutations in *RIT1*. We provide additional functional and computational data in conjunction with a zebrafish model to support the importance of increased MEK-ERK signaling in the development of the human RIT1 phenotype.

MATERIALS AND METHODS

Subjects

Following written informed consent, 3–10 ml EDTA blood was drawn from the patients and their parents, respectively. In addition, a skin biopsy was taken from patient 1. Informed consent was obtained from families regarding publication of photographs.

Methods

Methods for whole exome and Sanger sequencing, plasmid construction, cell transfection, western blotting, protein expression and signal transduction, zebrafish experiments and 3D modeling are noted in detail in the supplement.

RESULTS

Using whole exome sequencing (WES), we identified a heterozygous missense, predicted pathogenic variant in *RIT1* (c.270G>C [p.Met90Ile] (Figure 1), in patient 1, which was confirmed by bidirectional Sanger sequencing. The variant was absent in both parents. Additionally, 15 patients with a clinical phenotype suggestive of a RASopathy, were screened for mutations in *RIT1*. A 15-year-old girl (patient 2) was identified, carrying a *de novo* missense mutation in *RIT1* (c.170C>G [p.Ala57Gly]) (Figure 1). Neither mutation was listed in the dbSNP139 database, the 1,000 Genome database or the Human Gene Mutation Database (HGMD®). Interestingly, p.Met90Ile is listed in the COSMIC (Catalogue Of Somatic Mutations In Cancer, identifier: 357927) as somatic mutation in lung cancer and hematopoietic malignancies.

Patient 1

The boy was born at 39 weeks of gestation to healthy, non-consanguineous parents via C-section due to fetal distress following a pregnancy complicated by pre-eclampsia and polyhydramnios. The 33-year-old mother and 45-year-old father are of Cuban and Colombian descent, respectively. Apgar scores were 1/5/8. The boy’s birth parameters were

Author Manuscript Author Manuscript Author Manuscript Author Manuscript

at or above the 90th centile for gestational age: birth weight: 5.14 kg (>97th centile), birth length: 53.5 cm (90th centile) and head circumference (HC): 38.5 cm (>90th centile). He developed feeding difficulties and gastroesophageal reflux, which eventually required Nissen fundoplication and a gastric tube insertion. Facial dysmorphism included low set, posteriorly angulated ears, down-slanting palpebral fissures, anteverted nares with a depressed, broad nasal bridge, full lips with tented upper lip and sparse scalp hair, eyelashes and eyebrows (Figure 1), redundant skin with deep palmar and plantar creases and generalized muscular hypotonia. A postnatal cardiac echo showed a transient ductus arteriosus, transient patent foramen ovale, multiple small ventricular septal defects, mild pulmonary stenosis and concentric hypertrophic cardiomyopathy. At re-evaluation at age 3, he was diagnosed with lymphangioedema of the left lower extremity, expanding the extent of the phenotype (Figure 1). His growth is currently between the 5th and 10th centile and he continues to have delayed speech and fine motor development.

Patient 2

This girl was born at 34 weeks of gestation by C-section due to fetal distress to healthy non-consanguineous Caucasian parents. The pregnancy was complicated by cystic hygroma and cardiac hypertrophy. Her birth parameters were at or above the 90th centile: weight: 2.96 kg (>90th centile), length: 49 cm (90th centile). Her neonatal course was complicated by feeding difficulties requiring use of a nasogastric tube. A cono-ventricular septal defect was surgically repaired at the age of 4 months, and biventricular hypertrophy with right and left ventricular outflow tract obstruction was noted. A unilateral congenital cataract was surgically removed. Her early development was reportedly slightly delayed. At 15 years of age her performance was at grade level, with some adjustments for reading and vision issues. HC was 53.5 cm (<2 SD of mean for age), height 149 cm (<3rd centile; 50th centile for 11.5 years) and weight 37.1 kg (<3rd centile; 50th centile for age 11 years). Her height was at the 10th–25th centile between age 7 and 10 years. Facial features were consistent with Noonan syndrome with thick and curly hair, nystagmus, down-slanting palpebral fissures with bilateral ptosis, hypertelorism, and bilaterally low-set ears (Figure 1). Her neck was webbed and she had very mild pectus excavatum (Table 1).

Western blot analysis

There is no difference in atomic mass of total RIT1 protein between the normal control and the p.Met90Ile mutant present in patient 1 (data not shown).

Zebrafish *RIT 1* model

At tailbud stage (11 hours post fertilization, hpf), embryos injected with RIT1 variants (either 350 pg p.Met90Ile or 700 pg p.Ala57Gly) were malformed, with yolk sacs compressed in the dorsal-ventral axis. By contrast, WT RIT1 (wild-type RIT1, 350 or 700 pg) injected embryos showed normal round yolks typical of uninjected control embryos (Figure 2).

At 24 and 48 hpf, there was a range of phenotypes seen in embryos injected with the *RIT1* variants (Figure 2). Embryos injected with either human *RIT1* variant exhibited craniofacial abnormalities with altered eye morphology as the most obvious feature. Eye phenotypes

Author Manuscript Author Manuscript Author Manuscript Author Manuscript

were variable but included coloboma (failure of the eye's choroid fissure to fuse), smaller eyes and ventrally fused eyes or, in most severely malformed fish, cyclopia. Injection of human *RIT1* variants also altered the heart and pericardial sac. Heart ventricles were elongated, especially in embryos with acute pericardial edema. It was not uncommon to observe pooling of the blood in the heart cavity ventral to the ventricles (Figure 2).

MEK-ERK signaling in PC6 cells

Both p.Met90Ile (patient 1) and p.Ala57Gly (patient 2) *RIT1* substitutions induced phosphorylation of MEK and ERK, to levels that were comparable to those seen with p.Gln79Leu *RIT1* expression (Figure 2).

Mutant RIT1 3D model

The protein model of RIT1, built on a highly similar domain of HRAS shows p.Met90 buried within a cluster of completely conserved residues. p.Ala57 is located in the effector loop of RIT1, homologous to the effector domain in other *RAS* genes involved in binding and activation of select downstream effectors (Figure 1C, D). Additional simulation data about the structural impact of the p.Met90Ile mutation are reported as supplement.

DISCUSSION

RASopathies comprise a clinically diverse group of conditions caused by mutations in the RAS-MAPK signaling pathway. Next generation sequencing has facilitated the recent identification of novel disease genes, such as *RIT1* (3). We used WES in our index patient with a clinical phenotype suggestive of a RASopathy to identify a *de novo* pathogenic mutation in *RIT1* with subsequent identification of a 15-year-old girl who also carried a *de novo* pathogenic mutation in *RIT1* (Figure 1).

Since *RIT1* shares more than 50% sequence identity with other *RAS*-genes, such as *HRAS*, *KRAS* and *NRAS* that are associated with RASopathies, it is plausible that variants in *RIT1* cause a similar clinical phenotype (3,4,5). The two mutations we identified cause amino acid substitutions located within highly conserved regions common to all RAS family GTPases, including the G2 domain (p.Ala57Gly), and the switch II region (p.Met90Ile) with both residues being highly conserved throughout evolution. Both mutations were absent in several hundred control alleles and in exome and/or SNP databases, although they were reported but not functionally characterized by Aoki et al. in their series of RIT1 patients (3). The clinical phenotypes of the two patients with RIT1 mutations reported here differ from those reported by Aoki and colleagues, although there is phenotypic overlap (Table 1).

We show for the first time that the RIT1 variants p.Ala57Gly and p.Met90Ile are capable of enhancing ERK 1/2 signaling (Figure 2), supporting their role in RAS-MAPK-pathway activation.

RIT1 variants introduced into NIH3T3 fibroblasts enhance transactivation of *ELK1*, a member of the ETS oncogene family (9). ELK1 activation requires phosphorylation of its C-terminal DEF domain by ERK 1/2. ERK 1/2 has numerous cytosolic and nuclear targets in addition to ELK1. Other previously identified RASopathy genes are located further

Author Manuscript Author Manuscript Author Manuscript Author Manuscript

upstream in the pathway, interacting at several different locations in the cytosol. Previously reported mutations result in activation of the RAS-MAPK pathway, either by increasing RAS-GTP levels or by promoting ERK activity downstream of RAS (2).

Since ERK 1/2 are direct final effectors of the RAS-MAPK-pathway and are activated by MEK-mediated phosphorylation, we chose to directly examine the effect of *RIT1* variants on ERK 1/2, rather than use ELK1 as a surrogate for monitoring ERK pathway activity. Observing only ELK1 activity is insufficient, because ELK1 is only one of many of ERK1/2 targets (10). Other modulating factors could take effect in the signaling cascade, distorting the observed alterations.

Though we demonstrated that RIT1 is able to activate ERK 1/2, the mechanisms as well as direct binding partners remain unknown. RIT1 activates ERK-MAPK cascades in a BRAF-dependent fashion, promoting neuronal cell differentiation and survival in PC6 cells. These findings gave rise to the claim that RIT1 interacts with the upstream effector BRAF and that the latter might mediates ERK 1/2 activation. However, further studies are needed to delineate the pathogenic function.

The precise mechanism by which the identified mutations contribute to constitutive activation of RIT1 remains unclear. The protein model of RIT1, built on a highly similar domain of HRAS shows p.Met90 buried within a cluster of completely conserved residues suggesting that the p.Met90Ile mutation might have negative impact on the proper folding and structure of the domain. It also belongs to the switch II region, implicating the activation of RAS proteins. However, p.Met90 is positioned too far away from the ligand-binding pocket to exert an effect by its modification. It is possible that the variation to the slightly more hydrophobic isoleucine increases the barrier for conformational change to the inactive state upon GTP hydrolysis. An alternative possibility is that p.Met90Ile, and even more so p.Ala57Gly, a mutation that removes a surface accessible side chain, modify the interaction with an upstream regulator by changing the shape of the protein surface (Supplement). Since the activity of a RAS-like domain hinges on a statistical balance between GEF and GAP activity, tilting that balance by modifying the interaction propensity for either of the two can constitutively increase the signaling on the systemic level rather than constitutively activating the RAS domain itself. Further biochemical studies are needed to understand the mechanics of the observed activation.

Injecting zebrafish at the one-cell stage with either *RIT1* variant resulted in characteristic phenotypic findings. Some findings are comparable to other RASopathy zebrafish models, including elongated, dorso-ventrally compressed embryos, malformed yolks and a shortened body axis. In contrast to *NRAS* injected fish, which show wide-set eyes indicated by an increased ceratohyal angle (11), *RIT1* variant injected fish had narrowed eyes and in most severe cases cyclopia. In our experiments and the Japanese study (3), heart malformations resulted in elongated cardiac ventricles, whereas *HRAS* mutant fish showed smaller hearts and cardiac wall thickening. In conclusion, *RIT1* mutant fish recapitulate the human phenotype thus characterizing the functional role of *RIT1* in RASopathy pathogenesis. However, differences in morphology in mutant *BRAF*, *MEK*, *HRAS* and *NRAS* injected fish reflect the heterogeneity observed in human RASopathies. Introduction of continuous low-

Author Manuscript Author Manuscript Author Manuscript Author Manuscript

level MEK inhibition in mutant *BRAF* zebrafish resulted in an ameliorated phenotype underscoring the importance of MEK in the mechanistic context of RASopathies (12).

Supplementary Material

Refer to Web version on PubMed Central for supplementary material.

Acknowledgments

We are most grateful to the participating families and physicians who provided samples from patients with RASopathies. This work was supported by the National Multiple Sclerosis Society [NMSS-RG 4680A1/1 to J.L.M.], the National Institutes of Health [NIH-NS045103 to D.A.A., NIH-NIGMS-P20GM103464 and NIH-P20GM103446 to K.S.], the University of Kentucky Research Professorship to D.A.A., the Nemours Foundation Award to K.W.G. and the GeneSpotLight Foundation Award to O.A.B.

References

1. Yamamoto GL, Aguena M, Gos M, Hung C, Pilch J, Fahiminiya S, et al. Rare variants in SOS2 and LZTR1 are associated with Noonan syndrome. J Med Genet. 2015 Epub ahead of print.
2. Pierpont ME, Magoulas PL, Adi S, Kavamura MI, Neri G, Noonan J, et al. Cardio-facio-cutaneous syndrome: clinical features, diagnosis, and management guidelines. Pediatrics. 2014; 134(4):e1149–62. [PubMed: 25180280]
3. Aoki Y, Niihori T, Banjo T, Okamoto N, Mizuno S, Kurosawa K, et al. Gain-of-Function Mutations in RIT1 Cause Noonan Syndrome, a RAS/MAPK Pathway Syndrome. Am J Hum Genet. 2013; 93(1):173–180. [PubMed: 23791108]
4. Bertola DR, Yamamoto GL, Almeida TF, Buscarilli M, Jorge AA, Malaquias AC, et al. Further evidence of the importance of RIT1in Noonan syndrome. Am J Med Genet. 2014; 164(11):2952–2957. [PubMed: 25124994]
5. Gos M, Fahiminiya S, Poznański J, Klapecki J, Obersztyn E, Piotrowicz M, et al. Contribution of RIT1 mutations to the pathogenesis of Noonan syndrome: Four new cases and further evidence of heterogeneity. Am J Med Genet. 2014; 164(9):2310–2316. [PubMed: 24939608]
6. Chen PC, Yin J, Yu HW, Yuan T, Fernandez M, Yung CK, et al. Next-generation sequencing identifies rare variants associated with Noonan syndrome. Proc Natl Acad Sci USA. 2014; 111(31): 11473–11478. [PubMed: 25049390]
7. Lee CH, Della NG, Chew CE, Zack DJ. Rin, a neuron-specific and calmodulin-binding small G-protein, and Rit define a novel subfamily of ras proteins. J Neurosci. 1996; 16(21):6784–6794. [PubMed: 8824319]
8. Cherfils J, Zeghouf M. Regulation of small GTPases by GEFs, GAPs, and GDIs. Physiol Rev. 2013; 93(1):269–309. [PubMed: 23303910]
9. Cai W, Rudolph JL, Harrison SM, Jin L, Frantz AL, Harrison DA, Andres DA. An evolutionarily conserved Rit GTPase-p38 MAPK signaling pathway mediates oxidative stress resistance. Mol Biol Cell. 2011; 22(17):3231–3241. [PubMed: 21737674]
10. Besnard A, Galan-Rodriguez B, Vanhoutte P, Caboche J. Elk-1 a Transcription Factor with Multiple Facets in the Brain. Front Neurosci. 2011; 5:1–11. [PubMed: 21390287]
11. Runtuwene V, van Eekelen M, Overvoorde J, Rehmann H, Yntema HG, Nillesen WM, et al. Noonan syndrome gain-of-function mutations in NRAS cause zebrafish gastrulation defects. Dis Model Mech. 2011; 4(3):393–399. [PubMed: 21263000]
12. Anastasaki C, Rauen KA, Patton EE. Continual low-level MEK inhibition ameliorates cardio-facio-cutaneous phenotypes in zebrafish. Dis Model Mech. 2012; 5(4):546–552. [PubMed: 22301711]

Author Manuscript Author Manuscript Author Manuscript Author Manuscript

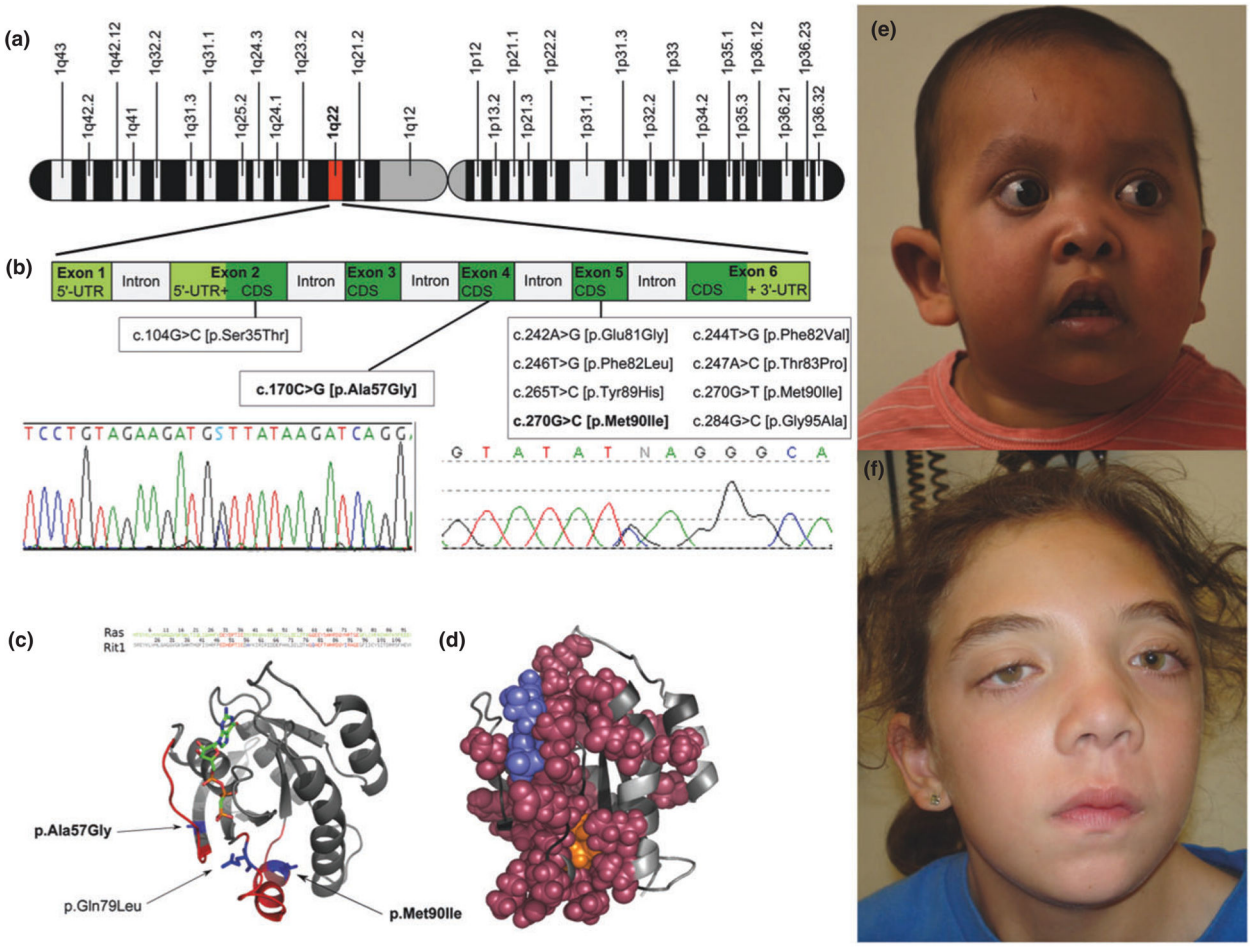

Figure 1. Chromosomal position (A), sequence chromatograms and published *RIT1* mutations (B) and protein structure of described RIT1 mutations (C and D). E: Patient 1 (2 years)

Note facial dysmorphism including low set, posteriorly angulated ears, down-slanting palpebral fissures, anteverted nares with a depressed, broad nasal bridge, full lips with tented upper lip and sparse scalp hair, eyelashes and eyebrows. At the follow up the patient developed lymphangioedema of the lower extremity, adding a novel feature to the phenotype. **F: Patient 2 (15 years):** Note facial features consistent with Noonan syndrome with thick and curly hair, down-slanting palpebral fissures with bilateral ptosis, hypertelorism, and bilaterally low-set ears.

Author Manuscript
Author Manuscript
Author Manuscript
Author Manuscript

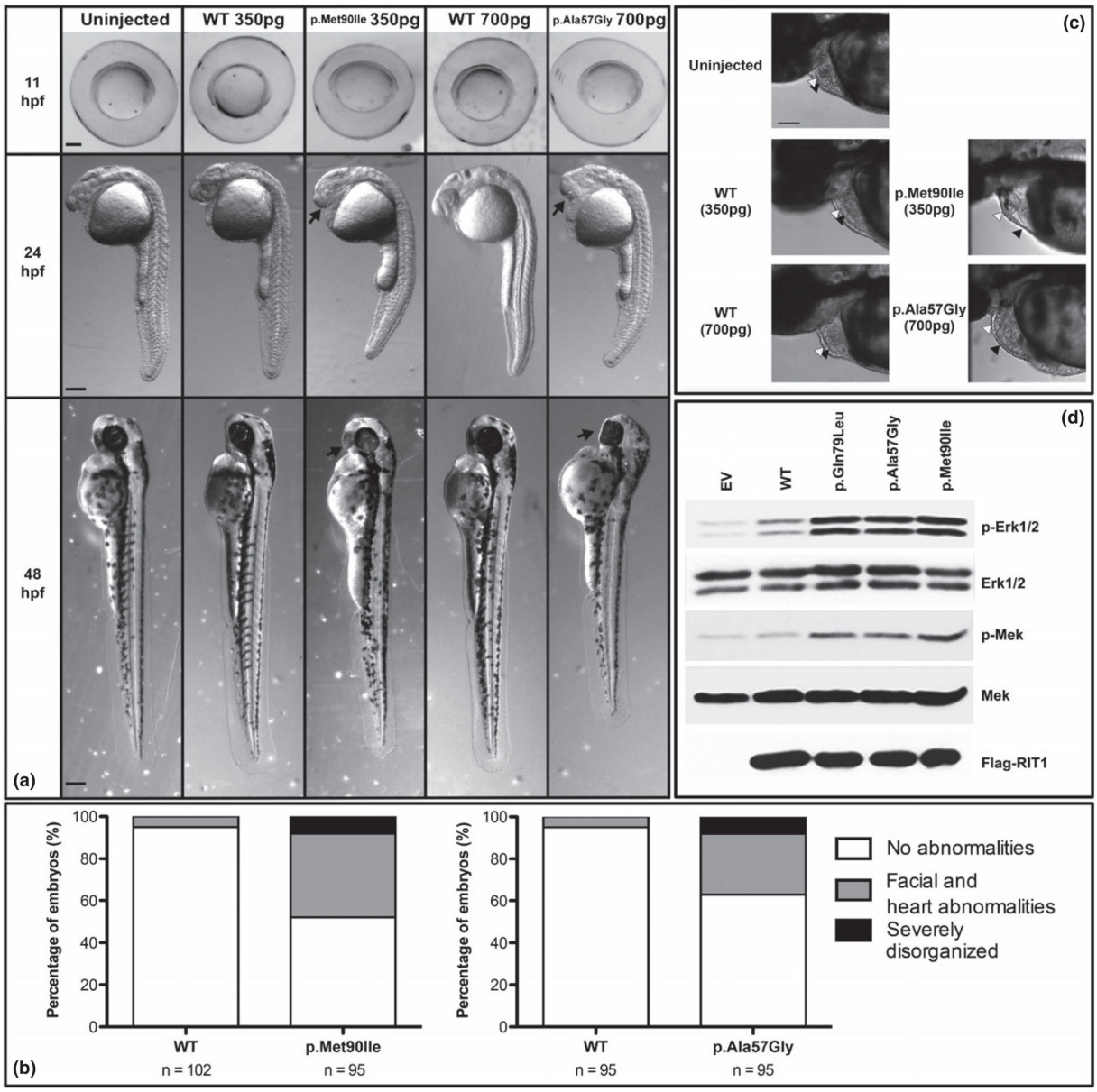

Figure 2. RIT1 variants alter zebrafish embryo morphogenesis (A)

Zebrafish embryos were injected at the one-cell stage with WT (350 pg - 2nd column; 700 pg - 4th column), p.Met90Ile (350 pg - 3rd column), or p.Ala57Gly (700 pg - 5th column) human *RIT1* RNA and morphologies were compared at 11 (top row), 24 (second row), and 48 hpf (bottom row) to un-injected controls (1st column). At tailbud stage (11 hpf, lateral view, heads to the left), RIT1 variant injected embryos appear oblong compared to WT RIT1 injected embryos and un-injected controls. At both 24 and 48 hpf, RIT1 variant injected larvae have small or cyclopic eyes, altered head structure, and malformed yolks compared to WT RIT1 injected embryos and un-injected controls. Red arrows indicate craniofacial abnormalities. Scale bars represent 200 mm. **Percentages of RIT1 injected zebrafish embryos presenting with morphological abnormalities at 48–52 hpf (B).**

Author Manuscript Author Manuscript Author Manuscript Author Manuscript

Embryos were injected at the one cell stage with 350 pg of RNA encoding either WT RIT1 (left) or p.Met90Ile (right); (700 pg of RNA encoding either WT RIT1 (left) or p.Ala57Gly (right). n = total number of embryos produced from at least 2 separate matings. Morphological abnormalities are scored for degree of severity: less severe phenotypes were limited to craniofacial and heart abnormalities (gray) while severe phenotypes included cyclopia, with a dysmorphic body plan often associated with a shortened anterior/posterior axis (black). **RIT1 variants and cardiac development in zebrafish embryos (C).** Injection of human RIT1 variants altered the heart and pericardial sac. Heart ventricles were elongated, especially in embryos that also exhibited acute pericardial edema. It was also not uncommon to observe pooling of the blood in the heart cavity ventral to the ventricles. Arrowheads indicate heart chambers: black; atrium, white; ventricle. Scale bars represents 100μm.

MEK-ERK signaling in PC6 cells (D). Mutated RIT1 induces MEK/ERK activation. Western blot of PC6 cell lysates following expression of wild-type (WT), mutant RIT1 (p.G79L, p.Ala57Gly, p.Met90Ile) or vector control (EV). Antibodies used detect phosphorylated MEK (p-MEK), phosphorylated ERK 1/2 (p-ERK), Flag tag (RIT1), or total MEK or ERK 1/2 as a loading control. Data shown are representative of a least three independent experiments.

Author Manuscript Author Manuscript Author Manuscript Author Manuscript

Clin Genet. Author manuscript; available in PMC 2017 March 01.

Table 1

Clinical phenotype in patients with *RIT1* mutations

	Noonan (RIT1)					
Clinical Findings	**Patient 1**	**Patient 2**	**Aoki et al. (17)**	**Bertola et al. (18)**	**Gos et al. (19)**	**Chan et al (20)**
Sex	M	F	8F/9M	2F/4M	4F	3F/1M
Ethnicity	Cuban	Caucasian	Japan	Brazil	Poland	?
Age	2y	15y	0–15y (mean 6y)	2–28y (mean 18.3y)	5.5–17.5 (mean 10.5y)	2–46 (mean 22y)
RIT1 mutations found	p.Met90Ile	p.Ala57Gly	p.Ser35Thr, p.Ala57Gly, p.Glu81Gly, p.Phe82Val, p.Phe82Leu, p.Thr83Pro, p.Tyr89His, p.Met90Ile, p.Gly95Ala	p.Ser35Thr, p.Ala57Gly, p.Phe82Leu, p.Gly95Ala	p.Phe82Val, p.Met90Ile, p.Gly95Ala	p.Ala57Gly, p.Ala77Pro, p.Phe82Val, p.Gly95Ala
Prenatal abnormalities			8/16		2/2	
Cystic hygroma	−	+	1/16	1/6	1/2	
Polyhydramnios	+	Not known	4/16	1/6		
Pleural effusion/chylothorax			2/16		1/2	
increased nuchal translucency			2/16		1/2	
Cardiac defect	+ (small aortic arch)				1/2	
Placental abruption			1/16		1/2	
Perinatal/Neonatal parameters						
Preterm delivery	−	+	−	1/6		
Increased birth weight	+	+	7/16 (>90%ile)		2/4 (>95%ile)	
Birth weight	5.14kg					
Increased birth length (>95%ile)					3/4	
Birth length	53.5cm					
mean Apgar 1′	1				5.5	
Hyperbilirubinemia			1/17		3/4	
Chylothorax			2/16			
Congenital pulmonitis					2/4	
Respiratory insufficiency	+ (tachypnoe, CPAP)		1/16 (TTN)		3/4	

Author Manuscript Author Manuscript Author Manuscript Author Manuscript

Noonan (RIT1)						
Clinical Findings	**Patient 1**	**Patient 2**	**Aoki et al. (17)**	**Bertola et al. (18)**	**Gos et al. (19)**	**Chan et al (20)**
Growth parameters						
Short stature	+	+	3/14	2/6	1/4 (3%ile)	3/4
Poor weight gain Feeding difficulties	+		5/11		4/4	
Craniofacial abnormalities						
Relative(?) Macrocephaly	−	−	7/13	4/6		
Typical facies			14/17	6/6	4/4	3/4
Hypertelorism	+		13/17		4/4	
Ptosis	+	+	10/16		1/4	
Epicanthal folds			11/16		3/4	
Blue irides					2/4	
Downslanting palpebral fissures	+	+	11/17		3/4	
Low-set ears	+	+	11/16		4/4	
Thickened Helix	+		1/16 (earlobe)		4/4	
Deep philtrum	+				3/4	
Myopathic Face					2/4	
Short/Webbed neck	−	+	10/15	6/6	4/4	
Low posterior hairline					4/4	
Cardiovascular abnormalities						
Pulmonary or pulmonary valve stenosis	+	+	11/17	5/6	4/4	4/4
Mitral/tricuspid valve anomaly	+	+	2/17	N/A		1/4
ASD/VSD	+	+	7/16	2/6	3/4	2/4
Hypertrophic cardiomyopathy	+	+	12/17	2/6	2/4	−
Patent ductus arteriosus	+		2/16	1/6	1/4	
Arrhythmia	+		1/16 (PVC)			1/4 (aFib)
Moyamoya			1/17			
Lymphangioedema	+ (left leg)	−			2/4	
Musculoskeletal deformities						
Scoliosis				1/6	1/4	
Pectus deformity			2/13	3/6	3/4	

Author Manuscript Author Manuscript Author Manuscript Author Manuscript

Noonan (RIT1)						
Clinical Findings	**Patient 1**	**Patient 2**	**Aoki et al. (17)**	**Bertola et al. (18)**	**Gos et al. (19)**	**Chan et al (20)**
Low muscle tone	+		1/17	3/6	3/4	
Ectodermal findings						
Curly hair			5/15	4/5	1/4	
sparse scalp hair	+					
sparse eyebrows/eyelashes	+					
Hyperpigmentation			6/12	−	1/4	
Hyperelastic skin			4/10	2/5		
Wrinkled palms and soles	+	−	5/9	3/5		
Ekzema			2/11			
Hyperkeratosis piliaris			3/10		−	
Intellectual or developmental delay	+	+	1/11 (IQ<70)	−		1/4
Speech delay			1/17	−	2/4	
Learning difficulty		+		−	2/4	
Severe/complex	+			−	1/4	
Motor delay			2/17	−		

Phenotypic spectrum in patients with *RIT1* mutations compared to patients with Noonan syndrome due to mutations in other genes of the RAS-MAPK pathway. M = male; F = female; y = years; CPAP = Continuous positive airway pressure; TTN = Transient tachypnea of the newborn; PVC = Premature ventricular contraction; aFib = Atrial fibrillation; bilat = bilateral; ALL = Acute lymphatic leukaemia; VUR = Vesicoureteral reflux; SLE = Systemic lupus erythematosus;